PERFORMANCE OF HIGH-LEVEL AND LOW-LEVEL CONTROL FOR COORDINATION OF MOBILE ROBOTS

Sisdarmanto Adinandra, Jurjen Caarls, Dragan Kostić and Henk Nijmeijer
Dept. of Mechanical Engineering, Eindhoven University of Technology, PO Box 513 5600MB, Eindhoven, The Netherlands

Keywords: Coordinated Control, Non-holonomic Systems, High-level and Low-level Control, Collision Avoidance, Performance Evaluation.

Abstract: We analyze performance of different strategies for coordinated control of mobile robots. By considering an environment of a distribution center, the robots should transport goods from place A to place B while maintaining the desired formation and avoiding collisions. We evaluate performance of two collision avoidance strategies, namely a high-level and low-level collision avoidance approach, each using different feedback information and update rate. As performance measure we take into account the time to accomplish the transportation task and the tracking errors of the robots. Evaluation is done in several experiments with seven mobile robots.

1 INTRODUCTION

A group of mobile robots can be used to realize spatially distributed transportation tasks in a distribution center. When several robots are employed in a shared environment, then motion coordination and cooperation between these robots can be introduced in order to increase robustness in the execution of their tasks.

Transportation in a distribution center is typically carried out by means of conveyors. Unfortunately, a failure in a single conveyor can disable a part of the transportation. To increase robustness of transportation, one can introduce redundant conveyers. This solution requires extra investments and occupies additional space. An appealing alternative is to substitute conveyers with mobile robots (Giuzzo, 2008). Unlike conveyers, the robots can dynamically alter their trajectories to avoid obstacles and complete assigned tasks. In addition, if one robot fails, its task can be delegated to another one. While engaging a number of mobile robots simultaneously, efficient robot coordination and cooperation control strategies are required to achieve high throughput in transportation of goods without collisions.

In the distribution center, planning and scheduling tasks are normally done in a centralized way. A high-level planning system decides which customers orders must be executed, together with the decision on how the tasks must be accomplished, see e.g. (van den Berg, 1999) and (Gu, *et al.,* 2007). Whereas this centralized approach can provide the optimal throughput in the absence of uncertainties, it can show quite some weaknesses in exceptional situations, such as when unexpected obstacles appear or when unknown disturbances start affecting the robots. In such situations, re-planning must be accomplished with time limitations that often lead to transportation plans that are not optimal in terms of the throughput. A viable alternative to the centralized approach is to facilitate negotiations among the robots and the supervisor which assigns the tasks. Through negotiation, the robots and the supervisor can dynamically adapt the transportation plans such as to make them less sensitive to different types of failures. The result might not have the optimal throughput, but it will likely bring higher robustness in comparison with the centralized approach. The high level coordination can be solved, for instance, using the holonic approach (Giret and Botti, 2004), (Moneva, *et al.,* 2009). Another example of the high-level coordination is decentralized control of Automated Guided Vehicles for distribution centers (Farahvash and Boucher, 2004), (Weyns, *et al.,* 2005*)*. In both works, a multi agent system is proposed for transportation planning, distribution of tasks, and collision avoidance.

At the layer of low-level control of individual

Adinandra S., Caarls J., Kostić D. and Nijmeijer H. (2010).
PERFORMANCE OF HIGH-LEVEL AND LOW-LEVEL CONTROL FOR COORDINATION OF MOBILE ROBOTS.
In *Proceedings of the 7th International Conference on Informatics in Control, Automation and Robotics*, pages 63-71
DOI: 10.5220/0002943800630071

mobile robots, various techniques of robot coordination and cooperation can be used to realize the transportation, such as leader-follower, behavior based, virtual structure, etc, (Ren and Beard, 2004), (Mastellone, *et al.*, 2008), (Sun *et al.*, 2009), (van den Broek *et al.*, 2009). In these approaches, the motion controllers achieve tracking of individual robot trajectories, on the one hand, and maintain the desired spatial formation between the robots, on another.

To the best of our knowledge, little research is devoted to performance comparison between the high-level and low-level control techniques. Some research have been conducted on performance comparison of different high-level techniques, see e.g. (Vis, 2004), (Le-Anh and De Koster, 2006), (Gu, *et al.*, 2010) and references therein. Furthermore, a quantitative evaluation of robustness of high-level control is still lacking, and no data are reported that illustrate how complicated it can be for the high-level control to find the optimal solution. Finally, there is scarce research on appropriate combination of high- and low-level control that can handle both effectiveness and robustness at the same time.

The lack of information has motivated us to quantitatively compare performance of high-level and low-level control of a group of mobile robots that perform a task which resembles coordinated transportation of goods in a distribution center. An ideal situation is simulated as a basis for comparison. We evaluate performance using relevant indicators, such as time to accomplish the task and errors in tracking the desired robot trajectories.

Two main contributions of this paper are: (*i*) suboptimal solutions for motion coordination of mobile robots, namely pure high-level and pure low-level coordination and (*ii*) experimental performance evaluation of these two strategies for completing transportation tasks in distribution center like environments.

This paper is organized as follows. In Section 2 we present necessary mathematical models and tools. Section 3 explains strategies to coordinate the motion of the mobile robots. Section 4 reports on experimental results and highlights the main findings of our performance analysis. Conclusions and discussion on future work are given in Section 5.

2 PRELIMINARIES

2.1 Unicycle Mobile Robots

We consider a group of m mobile robots that are described by the non-holonomic kinematic model of a unicycle, as depicted in Figure 1:

$$\begin{bmatrix}\dot{x}_i\\ \dot{y}_i\\ \dot{\theta}_i\end{bmatrix}=\begin{bmatrix}v_i\cos\theta_i\\ v_i\sin\theta_i\\ \omega_i\end{bmatrix}. \quad (1)$$

Here, v_i and ω_i are the forward and steering velocities, respectively, x_i and y_i are the Cartesian coordinates of the robot midpoint $\mathbf{O_i}$ in the world coordinate frame $\mathbf{O_{xy}}$, θ_i is the heading angle relative to the x-axis of the world frame, and $i\in\{1,2,3,\dots,m\}$. The reference trajectory of each robot i is given in the frame $\mathbf{O_{xy}}$:

$$\boldsymbol{P}_{ri}(t)=[x_{ri}(t)\quad y_{ri}(t)\quad \theta_{ri}(t)]^{\boldsymbol{T}}. \quad (2)$$

The trajectories of all mobile robots constitute a time-varying formation. An example is shown in Figure 2, where a platoon-like formation is adopted.

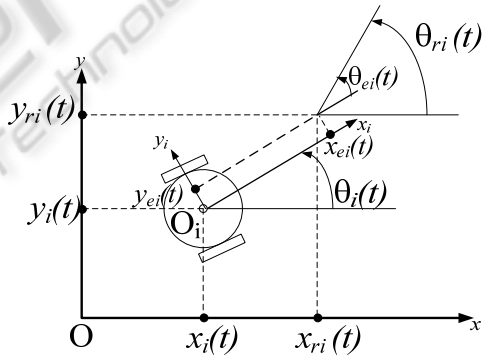

Figure 1: Configuration and error coordinates of a unicycle mobile robot.

2.2 Trajectory Tracking Control

To follow its own reference trajectory and to maintain the assigned formation, for each robot we propose the following control laws v_i and ω_i

$$v_i=v_{ri}\cos\theta_{ei}+k_{xi}x_{ei}+\sum_{j=1,j\neq i}^{m}s_x^{ij}k_x^{ij}x_{ej}\frac{(x_{ei}-x_{ej})}{\sqrt{1+x_{ei}^2+x_{ej}^2}}, \quad (3a)$$

$$\omega_i=\omega_{ri}+k_{yi}v_{ri}y_{ei}\frac{\sin\theta_{ei}}{\theta_{ei}}+k_{\theta i}\theta_{ei} \quad (3b)$$

$$+\sum_{j=1,j\neq i}^{m} s_y^{ij} k_y^{ij}\left(y_{ei}-y_{ej}\right)\frac{\sin\theta_{ei}}{\theta_{ei}}\sin\theta_{ej} + \sum_{j=1,j\neq i}^{m} s_\theta^{ij} k_\theta^{ij}\theta_{ej}\frac{\left(\theta_{ei}-\theta_{ej}\right)}{\sqrt{1+\theta_{ei}^2+\theta_{ej}^2}}.$$

where x_{ei}, y_{ei}, θ_{ei} are the tracking errors represented in the robot coordinate frame $\mathbf{O_{xiyi}}$

$$\begin{bmatrix} x_{ei} \\ y_{ei} \\ \theta_{ei} \end{bmatrix} = \begin{bmatrix} \cos\theta_i & \sin\theta_i & 0 \\ -\sin\theta_i & \cos\theta_i & 0 \\ 0 & 0 & 1 \end{bmatrix} \begin{bmatrix} x_{ri}-x_i \\ y_{ri}-y_i \\ \theta_{ri}-\theta_i \end{bmatrix}, \quad (3c)$$

k_x, k_y, k_θ are the design parameters that influence the performance of trajectory tracking, while $k_x^{ij}, k_y^{ij}, k_\theta^{ij}$ are the design parameters that influence formation keeping. Furthermore, $s_\alpha^{ij}, \alpha \in \{x, y, \theta\}$ is defined as follows:

$$s_\alpha^{ij} = \begin{cases} \mathrm{sgn}(\alpha_{ei}) & |\alpha_{ei}| \geq |\alpha_{ej}| \\ \mathrm{sgn}(\alpha_{ej}) & |\alpha_{ei}| < |\alpha_{ej}| \end{cases}. \quad (3d)$$

The control laws (3a,b) guarantee globally asymptotic tracking of $\boldsymbol{P}_{ri}(t)$ and represent a non-saturated version of the controller proposed in (Kostić, *et al.*, 2009) and (Kostić, *et al.*, 2010).

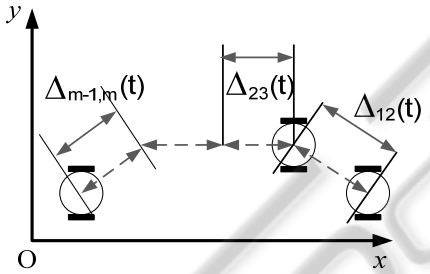

Figure 2: An example of a convoy-like, time-varying formation.

2.3 Penalty Functions

We introduce a set P_γ of continuous, monotone and bounded penalty functions indexed by a constant parameter $\gamma \in \mathbb{R}^+$ (Kostić, *et al.*, 2009):

$$P_\gamma = \{\delta_\gamma : \mathbb{R} \to \mathbb{R} \mid \delta \text{ is continous, monotone }, \; \delta_\gamma = \delta_{\gamma,min} \text{ if } x \in \mathbb{R}^+, \; \delta_{\gamma,min} \leq \delta_\gamma(x) \leq \delta_{\gamma,max} \text{ if } \gamma_{min} \leq x \leq \gamma_{max}, \; \delta_\gamma(x) = \delta_{\gamma,min} \text{ if } x \geq \gamma_{max}\}. \quad (4)$$

An example of a function in P_γ is

$$\delta_\gamma(x) = \begin{cases} \delta_{\gamma,max}, & x < \gamma_m \\ 1 - \Delta_\gamma\left(\lambda\left(x - \gamma_{min} - \frac{\sin\psi\,(x-\gamma_{min})}{\psi}\right)\right), & \gamma_{min} \leq x \leq \\ \delta_{\gamma,min}, & x > \gamma_m \end{cases} \quad (5)$$

where $\Delta_\gamma = \gamma_{max} - \gamma_{min}$ and $\psi = 2\pi / (\gamma_{max} - \gamma_{min})$.

3 HIGH-LEVEL AND LOW-LEVEL COORDINATION

To achieve transportation with high throughput and increase robustness to uncertainties, such as disturbances, all engaged robots have to cooperate. These robots have to coordinate their motions such as to avoid collisions and keep the sequence as assigned by the given formation.

In this research, we investigate the performance of two coordination methods, namely high-level coordination and low-level coordination. The coordination takes care of collision avoidance and keeping the desired robot sequence. Both aspects are very relevant for realization of transportation tasks in a distribution center environment.

3.1 High-level Coordination

The high-level method of coordination is implemented at the level of generating the reference trajectory (2) for each robot. This method assumes that the robots move from waypoint to waypoint (nodes) on a network of fixed path segments (edges). This network enables us to define spatial reference trajectories.

To accomplish a given transportation task, a timed desired trajectory along the desired path segments is generated by each robot. For collision avoidance it is needed to coordinate (predicted) intervals of appearance of the robots at intersecting segments. If these time intervals are well coordinated, then the absence of collisions is guaranteed as long as each robot accurately follows its own reference trajectory. In this case, the coupling gains k_x^{ij}, k_y^{ij} and k_θ^{ij} between robots in the control laws (3) have to be set to zero. Figure 3 illustrates this coordination method in a situation where trajectories of three robots intersect at junction J1.

The junction is represented by a group of intersecting path segments. Each segment brings a robot from one side of the junction to another. Therefore, the interval a robot occupies the junction

is marked by passing the beginning and ending waypoints of such a segment.

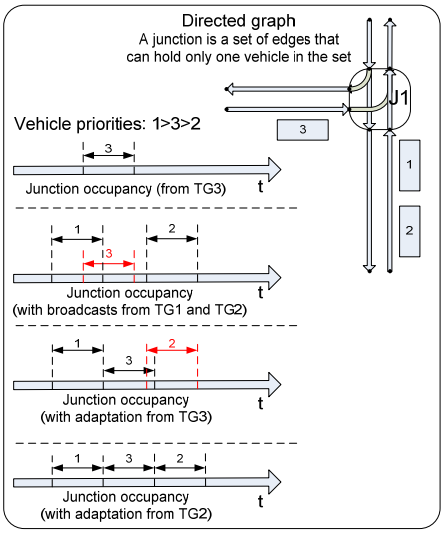

Figure 3: High-level coordination for collision avoidance.

At regular intervals, currently 1s, each robot broadcasts its occupation interval to other robots headed to J1. If overlap is detected, the robot of the highest priority will rebroadcast its occupation interval immediately to notify the other robots.

The robot of lower priority will postpone its arrival time at the junction until the leaving time of the robot of higher priority. Each robot adjusts its speed immediately such as to reach the junction at the correct time. The necessary speed is calculated and all passing times at the waypoints between the robot and the junction are adapted accordingly.

Similarly, the passing times after the junction should be changed too. From the junction segment on, the passing times are only adapted when the robot would require to exceed its speed limits. Once both the entering and leaving waypoint passing times on the junction are known, the robot broadcasts its new non-overlapping occupation interval, and waits again for incoming occupation intervals.

The priority of a robot is determined as the sum of the total time this robot has to wait for other ones, excluding those in front of it, and the expected time to enter the junction. This is similar to the first come first served priority scheme, which minimizes the queues in front of the junctions as well as the waiting times of the individual robots.

3.2 Low-level Coordination

The low-level coordination is implemented at the level of trajectory tracking control. To keep the correct robot sequence according to the desired spatial pattern, the coupling gains k_x^{ij}, k_y^{ij}, and k_θ^{ij} are set to positive non-zero values. With such gains, the control law (3) will be able to track the desired formation, e.g. as shown in Figure 2. Due to this coupling, the robots can recover their formation faster than their individual desired paths, thereby maintaining the desired sequence of robots better than without the coupling.

To gain more robustness to uncertainties, the reference forward velocity $v_{ri}, i \in \{1,2,3,\dots,m\}$, of each robot is also adjusted using the penalty functions from the set P_γ defined by (4). For each robot we determine the distance between its reference and actual position:

$$\Delta_{rp,i} = \sqrt{(x_{ri} - x_i)^2 + (y_{ri} - y_i)^2}. \quad (6)$$

If $\Delta_{rp,i} > \gamma_{min}$, then the desired forward velocity of each robot i is penalized as follows:

$$v_{ri} = v_{des,i} \prod_{j=1}^{m} \delta_{\gamma j}(\Delta_{rp,j}). \quad (7)$$

Here, $\delta_{\gamma j}$ is a penalty function from the set (4) and $v_{des,i}$ is the desired forward velocity. Using (7), if one robot is far from the assigned path, then the forward velocities of all robots are decreased in order to give the perturbed robot time to get back on its track. In this way, it will be easier to keep the correct sequence of the robots.

To avoid collisions, we make use of an Artificial Potential Field (APF) (Latombe, 1991). The reference trajectories of the robots facing collisions are online adapted using the APF, mimicking the approach in (Kostić, *et al.*, 2010). If $\boldsymbol{q}_i = (x_i, y_i)$ and $\boldsymbol{q}_j = (x_j, y_j)$, $i,j \in \{1,2,\dots,m\}$, are the Cartesian coordinates of the robots i and j, respectively, then an APF of robot i is:

$$V_i = \sum_{j=1, j\neq i}^{m} V_{i,j}(\boldsymbol{q}_i, \boldsymbol{q}_j) + \rho_{att}(\boldsymbol{q}_i, \boldsymbol{P}_{ri}), \quad (8)$$

where

$$\rho_{att}(\boldsymbol{q}_i, \boldsymbol{P}_{ri}) = \frac{1}{2} K_a((x_i - x_{ri})^2 + (y_i - y_{ri})^2), \quad (9)$$

$$V_{i,j}(\boldsymbol{q}_i, \boldsymbol{q}_j) = \begin{cases} K_o e^{-\frac{1}{2}\left(\frac{(x_i - x_j)^2}{\alpha} + \frac{(y_i - y_j)^2}{\beta}\right)}, & \|\boldsymbol{q}_i - \boldsymbol{q}_j\|_2 - rob_d < d_s \\ 0, \text{ elsewhere.} \end{cases} \quad (10)$$

Here, K_o and K_a are the gains of the repulsive and attractive fields, respectively, α and β are positive real numbers that determine the size of the detection region for the repulsive function, rob_d is the robot diameter, and d_s is the threshold of the detection region. When all obstacles are outside the detection region of robot i, its tracking controller tracks the trajectory $\boldsymbol{P}_{ri}(t)$. Inside the detection region, the low-level coordination modifies the trajectory as follows:

- Determine the Cartesian velocities that move the robot in the direction of the steepest descent of V_i (away from the obstruction):

$$\begin{bmatrix}\delta v'_{x,i}\\ \delta v'_{y,i}\end{bmatrix} = -\begin{bmatrix}\frac{\partial V_i}{\partial x_i}\\ \frac{\partial V_i}{\partial y_i}\end{bmatrix}, \delta v_i = \sqrt{\left(\delta v'_{x,i}\right)^2+\left(\delta v'_{y,i}\right)^2}. \quad (11)$$

- Update the reference trajectory such that collision avoidance is achieved at time-instant t_k:

$$x_{ri}(t_k) = x_i(t_{k-1}) + (t_k - t_{k-1})\delta v_i, \quad (12a)$$

$$y_{ri}(t_k) = y_i(t_{k-1}) + (t_k - t_{k-1})\delta v_i, \quad (12b)$$

$$\theta_{ri}(t_k) = \begin{cases}\text{atan}(\delta v'_{y,i}/\delta v'_{x,i}), & \text{if } \delta v_i > 0,\\ \theta_{ri}(t_{k-1}), & \text{if } \delta v_i = 0,\end{cases} \quad (12c)$$

$$v_{ri}(t_k) = \sqrt{\left(\delta v'_{x,i}\right)^2+\left(\delta v'_{y,i}\right)^2}, \quad (12d)$$

$$\omega_{ri}(t_k) = \frac{\theta_{ri}(t_k)-\theta_{ri}(t_{k-1})}{t_k - t_{k-1}}. \quad (12e)$$

4 EXPERIMENTS AND PERFORMANCE ANALYSIS

4.1 Scenario

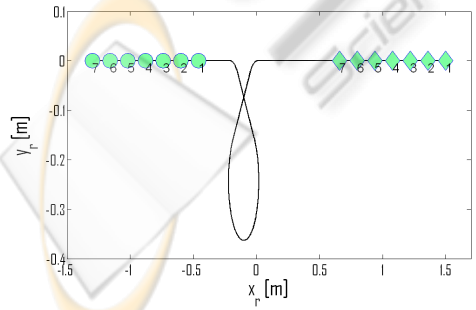

Figure 4: The experimental robot path. Symbols "o" and "◊" indicate the start and end positions of the robots, respectively.

To mimic a realistic transportation task in a distribution center, experiments are conducted according to the following scenario: a convoy of seven robots delivers goods along a path depicted in Figure 4. At one segment of this path, the front part of the convoy intersects with the part at the back; consequently, robot coordination is needed to avoid collisions between the robots and to keep the correct robot sequence. The desired forward velocity of each robot is 0.08 [m/s].

For performance evaluation, we use the following indicators:

1. The average of the travel times, $\overline{t_{tvrl}}$, that the robots consume to reach their target locations:

$$\overline{t_{tvrl}} = \frac{\sum_{i=1}^{7} t_{tvrl,i}}{7}. \quad (13)$$

2. The normalized total tracking error of all robots:

$$e_{xy,tot} = \sum_{i=1}^{7}\sqrt{\frac{1}{l}\sum_{k=1}^{l}\left(x_{ro,i}(t_k) - x_i(t_k)\right)^2 + \left(y_{ro,i}(t_k) - y_i(t_k)\right)^2}. \quad (14)$$

where t_k is the moment of collecting data, l is the number of data points in the experiment, $x_{ro,i}$ and $y_{ro,i}$ are the originally assigned robot reference, while x_i and y_i are the actual positions.

3. The normalized total formation error. In the experiments we use a platoon-like formation, which has a spatial pattern described by a time-varying Euclidean distance between the neighboring robots. For seven robots, the pattern can be described for $i \in \{1,2,3,4,5,6\}$ and $j = i + 1$, as follows:

$$\Delta_{rij}(t) = \sqrt{\left(x_{ro,i}(t) - x_{ro,j}(t)\right)^2 + \left(y_{ro,i}(t) - y_{ro,j}(t)\right)^2}. \quad (15)$$

We define the individual formation error by

$$\delta_{ij}(t) = \Delta_{rij}(t) - \Delta_{ij}(t), \quad (16)$$

where $\Delta_{ij}(t)$ is the actual Euclidean distance between the robots i and j. Thus, the normalized total formation error is given by:

$$\delta_{ij,tot} = \sum_{i=1}^{6}\sum_{j=i+1}^{7}\sqrt{\frac{1}{l}\sum_{k=1}^{l}\left(\delta_{ij}(t_k)\right)^2}. \quad (17)$$

For a total performance indicator, we take the summation of the three indicators proposed above with equal weight:

$$\sum_{perf} = \overline{t_{tvrl}} + e_{xy,tot} + \delta_{ij,tot}. \quad (18)$$

4.2 Experimental Set-up

Our experimental setup is depicted in Figure 5. We

use mobile robots, model e-puck (Mondala and Bonani, 2007), a camera as a localization device for getting the position and orientation of all robots, and a PC. The PC generates robot trajectories, processes camera images to get the actual pose of the robots, and runs the collision avoidance algorithms and tracking control laws for all the robots. The PC sends the control velocities to the robots via a BlueTooth protocol. This way of implementation is chosen due to the limiting processing power of the onboard robot processors and due to the limited bandwidth of the BlueTooth communication.

4.3 Experimental Results and Analysis

In the experiments, we use the following design parameters:

$$k_x = 0.4,\ k_y = 100,\ k_\theta = 0.5, \quad (19a)$$

$$k_x^{ij} = 0.06, k_y^{ij} = 10, k_\theta^{ij} = 0.00001, \quad (19b)$$

$$K_0 = 20,\ K_a = 10, \alpha = \beta = 0.05, \quad (19c)$$

$$d_s = 0.03\ [\text{m}],\ \Delta_{rij} = 0.14\ [\text{m}], \quad (19d)$$

$$\gamma_{min} = 0.05\ [\text{m}], \gamma_{max} = 0.5\ [\text{m}], \quad (19e)$$

$$\delta_{\gamma i}(\Delta_{rp,i})_{min} = 0.3,\ \delta_{\gamma i}(\Delta_{rp,i})_{max} = 1. \quad (19f)$$

The values of k_x, k_y, k_θ are chosen such that we have an accurate trajectory tracking. As for $k_x^{ij}, k_y^{ij}, k_\theta^{ij}$, the values will be zero if high-level coordination is active. When low-level coordination is active, the values are chosen such that we have strong coupling between the robots, especially in *x* and *y* direction.

As a basis for comparison, we simulate the case where the coupling terms in the control law (3) are enabled and collisions are allowed. In this unrealistic case, all the robots can travel without perturbation from the start to the end position, while keeping the formation. To account for realistic imperfections of the vision system used in experiments, we add simulated noise, drawn from a normal distribution with zero mean and standard deviation of ±0.005 [m] for *x* and *y*, and $\pm 0.5^0$ for θ, in accordance with the measurement noise of the real camera. The following results are obtained:

$$\overline{t_{tvrl}} = 36.06\ [\text{s}], e_{xy,tot} = 0.0024[\text{m}], \quad (20a)$$

$$\delta_{ij,total} = 0.0019[\text{m}], \sum_{perf} = 36.06\ 43[\text{-}]. \quad (20b)$$

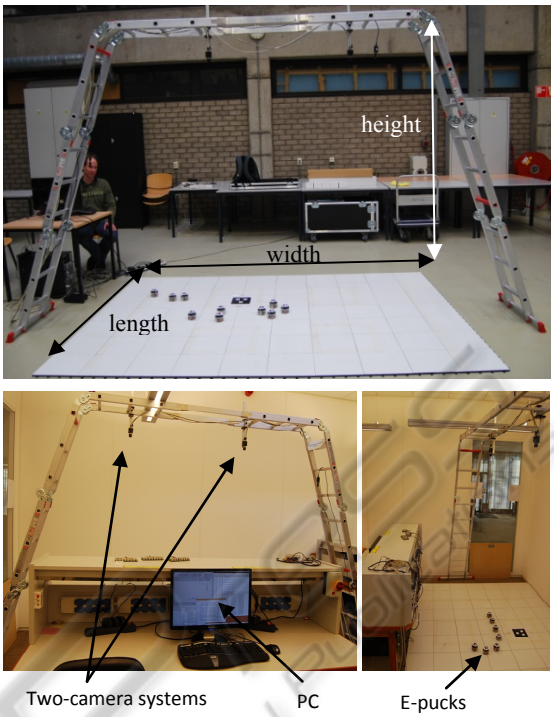

Figure 5: The experimental set-up.

The simulation results are used as a reference for comparison with data obtained from experiments. Tables 1a and 1b show statistics of all performance indicators obtained in ten repeated experiments, while Figure 6 shows a graphical representation of these statistics.

ANALYSIS. From the second column of Table 1a and Figure 6, we can see that the high-level coordination achieves the shortest average travel time with respect to other strategies. Thanks to negotiations among the robots in the high-level coordination, collision avoidance is achieved time-efficiently, which leads to short travel times.

Table 1a: Mean value and standard deviation of $\overline{t_{tvrl}}$ and $e_{xy,tot}$ in ten repeated experiments.

Strategies	Indicators			
	$\overline{t_{tvrl}}$[s]		$e_{xy,tot}$[m]	
	mean	Std	mean	Std
[1]HL	**36.06**	0	**0.105**	**0.00088**
[2]LL-1	38.939	1.920	0.907	0.4501
[3]LL-2	38.110	1.184	0.737	0.3277
[4]LL-3	38.633	1.024	0.885	0.2796
[5]LL-4	40.204	2.277	1.228	0.3470

[1]HL: high-level; [2]LL-1: low level, no coupling between robots [3]LL-2: low-level, all robots are mutually coupled; [4]LL-3: low-level, each robot is coupled to the leader robot, i.e. the first robot of the convoy, not vice versa; [5]LL-4: low-level, each robot is coupled to the robot in front of it, not vice versa.

Moreover, the travel time is identical to the one achieved under the ideal condition (20a). The given experimental result suggests that the high-level control yields time-optimal transportation while taking care of collision avoidance.

Table 1b: Mean value and standard deviation of $\delta_{ij,tot}$ in ten repeated experiments and Σ_{perf}.

Strategies	Indicators		
	$\delta_{ij,tot}$[m]		Σ_{perf}
	mean	std	
[1]HL	**0.0782**	0.00045	36.243200
[2]LL-1	0.0934	0.04390	39.939400
[3]LL-2	0.0853	0.02390	38.932299
[4]LL-3	0.0862	0.00770	39.604199
[5]LL-4	0.1170	0.05540	41.548999

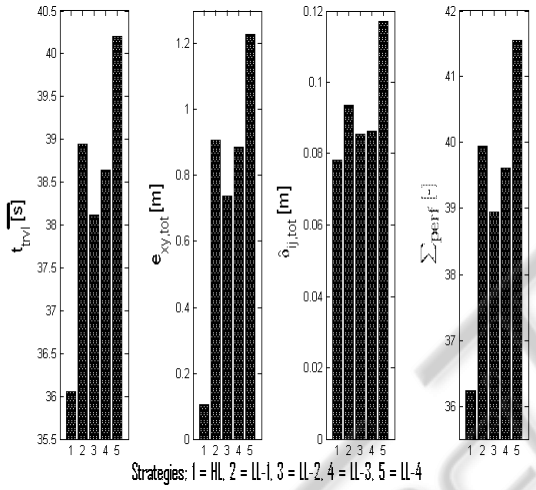

Figure 6: The mean values of $\overline{t_{tvrl}}$, $e_{xy,tot}$, $\delta_{ij,tot}$ from different coordination strategies and Σ_{perf}.

As for the low-level coordination, according to the second column of Table 1a and Figure 6, in all low-level coordination methods, the total travel time is longer than achieved using the high-level coordination. The online APF strategy does not utilize negotiations; a robot facing an imminent collision tries to move away from the obstacle. Time-optimality of such a collision avoidance algorithm is not guaranteed.

In our experiments, the lowest tracking errors are achieved using the high-level coordination. With modest uncertainties, this strategy ensures that each robot follows its own collision-free reference trajectory. Consequently, the difference between the actual and the desired robot trajectories remains small, which results in small tracking errors. This is in line with the observation that the shortest travel time is characteristic for the high level strategy. In addition, the way the high-level strategy solves the collision avoidance is also useful for formation keeping, as depicted in Figure 6.

When comparing the tracking errors, the low-level coordination strategies, all yield larger tracking errors compared to the high-level coordination. As expected, the tracking errors with coupling are slightly larger than without coupling. Having the couplings, a robot adapts its movement to other perturbed robots. In this way, the tracking control can keep the formation but by doing so, it decrease its own tracking performance. Despite the poor tracking error performance, as shown in Figure 6, introducing correct coupling helps the robots keep the formation.

If a decision needs to be made, a single measure is needed to base it on. Comparing the values of the total performance, we can observe that in our experiments, option LL-2 turns out to be the most suitable option for the low-level coordination method.

Overall, it appears that the high-level control is the most promising solution according to the total performance measure. However, this solution may fail in case of perturbations. The high-level strategy requires all robots to be in the correct position for a successful collision-free execution. If one robot is not at the correct position at some time instant, collisions may occur and the correct robot sequencing cannot be guaranteed.

The low-level coordination is inherently more robust to perturbations. Despite perturbations, the low-level coordination achieves collision avoidance and formation keeping. In the presence of perturbations, from the comparison of the indicators and considering the importance of formation, the fully coupled option (LL-2) seems to be the most appealing one. We show in Table 2 the minimum distances between the center points of all robots, measured from an experiment using the LL-2 strategy. During the experiment robot 4 was manually displaced from the platoon. Since the diameter of the robot is 0.07 [m], any value below 0.07 [m] implies a collision between robots. Table 2 shows no distances below 0.08 [m], so no collisions occurred.

Given experimental analysis brings us to the conclusion that it is not easy to find a single solution that scores best in terms of all performance indicators and is robust enough against uncertainties. There will be a set of solutions that are best, i.e. no better solutions exist in one performance indicator, without being worse in another. These solutions are called pareto-optimal solutions. One has to choose a

weighing between all indicators, as in the total performance indicator (18), to select the best one for a certain application.

Table 2: Minimum distances between the centers of all robots. $d_{ci,j}$ denotes the distance between robots i and j.

min $d_{ci,j}$[m]							
robot	1	2	3	4	5	6	7
1	-	0.08	0.08	0.09	0.16	0.09	0.08
2		-	0.08	0.17	0.23	0.19	0.14
3			-	0.08	0.17	0.20	0.18
4				-	0.08	0.09	0.17
5					-	0.08	0.08
6						-	0.08

The problem remains to find those pareto-optimal solutions. The high-level and low-level coordination strategies that we propose still can be improved and optimized in terms of all performance indicators, e.g. using larger safety distance for the high level method or having a smoother transition from normal to collision mode for the low level methods. Finding the true pareto-optimal solutions is probably not possible. However, from a set of solutions one can always remove the non pareto-optimal solutions, and choose from the remaining, best, ones.

5 CONCLUSIONS

We have experimentally evaluated the performance of different strategies for coordinated control of mobile robots. We have proposed high-level and low-level coordination methods and presented experimental results that illustrate the superior performance of the high-level method in terms of time efficiency and accuracy of tracking the desired robot trajectories. A serious limitation of the high-level coordination is the requirement for accurate tracking of the reference trajectories.

Even though the performance of the low-level coordination method is worse than that of the high-level coordination method, the low-level one is inherently more robust against uncertainties.

Given the results of our analysis, it seems interesting to analyze performance of combinations of different strategies, e.g., of high-level and low-level coordination methods. By combining more strategies, we may optimize more performance indicators and meet more requirements. Consequently, it needs to be investigated which combinations would lead to the pareto-optimal solutions.

ACKNOWLEDGEMENTS

This work has been carried out as part of the FALCON project under the responsibility of the Embedded Systems Institute with Vanderlande Industries as the industrial partner. This project is partially supported by the Dutch Ministry of Economic Affairs under the Embedded Systems Institute (BSIK03021) program.

REFERENCES

Berg, J. P. van den, 1999, A literature Survey on Planning and Control of Warehousing Systems, in *IIE Transactions*, Vol.31, pp. 751-762.

Broek, T. H. A. van den, van de Wouw, N., Nijmeijer, H. 2009, Formation Control of Unicycle Mobile Robots: a Virtual Structure Approach, in *Proc. IEEE Conf. on Decision and Control,* pp. 8238-8333.

Farahvash, P., and Boucher, T. O., 2004, A Multi-agent Architecture for Control of AGV Systems, in *Robotics and Computer Integrated Manufacturing*, Vol.20, pp. 473-483.

Giret, A., and Botti, V., 2004, Holons and Agents, in *J. of Intelligent Manufacturing*, Vol. 15, pp. 645-659.

Giuzzoa, E., 2008, Three Engineers, Hundred of Robots, One Warehouse, in *IEEE Spectrum,* Vol. 45. No. 7, pp. 26-34.

Gu, J., Goetschalckx, M., McGinnis, L. F., 2007, Research on Warehouse Operation: A Comprehensive review, in in *European Journal of Operational Research,* Vol. 177, pp. 1-21.

Gu, J., Goetschalckx, M., McGinnis, L. F., 2010, Reseach on Warehouse Design and Performance Evaluation: A Comrehensive review, in *European Journal of Operational Research,* Vol. 203, pp. 539-549.

Kostić, D., Adinandra, S., Caarls, J., Nijmeijer, H., 2009, Collision-free Tracking Control of Unicycle Mobile Robots, in *Proc. IEEE Conf. on Decision and Control,* pp. 5667-5672.

Kostić, D., Adinandra, S., Caarls, J., Nijmeijer, H., 2010, Collision-free Tracking Control of Unicycle Mobile Robots, Collision-free Motion Coordination of Unicycle Multi-agent Systems, *Accepted for American Control Conference 2010.*

Latombe, J. C., 1991, *Robot Motion Planning*, Kluwer Academic Publishers, Boston, MA.

Le-Anh, De Koster, M. B. M., 2006, A review of Design and Control of Automated Guided Vehicles Systems, in *European Journal of Operational Research,* Vol. 171, pp. 1-23.

Mastellone, S., Stipanović, D. M., Graunke, C. R., Intlekofer, K. A., and Spong, M. W., 2008, Formation Control and Collision Avoidance for Multi-agent Non-holonomic Systems: Theory and Experiments, in *Int. Journal of Robotics Research*, Vol.27, No. 1, pp. 107-126.

Mondala, F., Bonani, M., 2007, E-puck education robot, www.e-puck.org.

Moneva, H., Caarls, J., and Verriet, J., 2009. A Holonic Approach to Warehouse Control, in *Int. Conf. on Practical Applications of Agents and Multiagent Systems,* pp. 1-10.

Ren, W. and Beard, W., 2004, Decentralized Scheme for Spacecraft Formation via The Virtual Structure Approach, in *IEEE Proc. Control Theory Application 2004,* pp. 268-357.

Sun, D., Wang, C., Shang, W., Feng, G., 2009, A Synchronization Approach to Trajectory Tracking of Multiple Mobile Robots While Maintaining Time-Varying Formations, *IEEE Transactions on Robotics,* Vol.25, pp. 1074-1086.

Vis, I. F. A, 2004, Survey of Research in the Design and Control of Automated Guided Vehicle Systems, in *European Journal of Operational Research,* Vol. 170, pp. 677-709.

Weyns, D., Schelfthout, K., Holvoet, T., and Lefever, T., 2005, Decentralized Control of E'GV Transportation Systems, in *Autonomous Agents and Multiagent Systems, Industry Track (Pechoucek, M. and Steiner, D. and Thompson, S., eds.),* pp. 67-74.